


$a_0(1710)$ - $f_0(1710)$ mixing effect in the $D_s^+ \rightarrow K_S^0 K_S^0 \pi^+$ decayYu-Wen Peng,¹ Wei Liang^{1,*}, Xiaonu Xiong,¹ and Chu-Wen Xiao^{1,2,3,†}¹*School of Physics, Central South University, Changsha 410083, China*²*Department of Physics, Guangxi Normal University, Guilin 541004, China*³*Guangxi Key Laboratory of Nuclear Physics and Technology, Guangxi Normal University, Guilin 541004, China* (Received 8 February 2024; accepted 18 June 2024; published 22 August 2024)

With the measurements of the decay $D_s^+ \rightarrow K_S^0 K_S^0 \pi^+$ by the BESIII collaboration, we investigate this three-body weak decay via the chiral unitary approach for the final state interaction, where the resonances $S(980)$ and $S(1710)$ are dynamically reproduced with the interaction of eleven coupled channels, and the W -external and W -internal emission mechanisms are considered at the quark level. Besides, we also take into account the contribution from the P -wave resonance $K^*(892)^+$ and make a combined fit of the $K_S^0 K_S^0$ and $K_S^0 \pi^+$ invariant mass spectra measured by the BESIII collaboration. The fitted results show that the enhancement around 1.7 GeV in $K_S^0 K_S^0$ mass spectrum is overlapped with two visible peaks, indicating the mixing signal originated from the resonances $a_0(1710)$ and $f_0(1710)$ due to their different poles (masses). Thus, the decay $D_s^+ \rightarrow K_S^0 K_S^0 \pi^+$ is helpful to reveal their molecular nature with the mixing signal, which can be more precisely measured in the future.

DOI: [10.1103/PhysRevD.110.036013](https://doi.org/10.1103/PhysRevD.110.036013)**I. INTRODUCTION**

Because of the confinement and nonperturbative properties of quantum chromodynamics, the internal structure of the hadrons is a debated issue in the particle physics. Especially the properties of some resonances found in the experiments are challenging to be explained using the conventional quark model, such as $f_0(500)$, $f_0(980)$, $a_0(980)$, $\Lambda(1405)$, and so on. Note that the states $f_0(980)$ and $a_0(980)$ were found more than 50 years ago [1–3], of which the properties were under debate for a long time [4–17]. Both of them are generally assumed to be the $K\bar{K}$ molecule [10–17]. Thus, due to the equal masses of $f_0(980)$ and $a_0(980)$ close to the $K\bar{K}$ threshold, the $a_0(980)$ - $f_0(980)$ mixing effect was predicted more than 40 years ago [18]. Later, more theoretical work discussing the $a_0(980)$ - $f_0(980)$ mixing can be found in Refs. [19–27], and the experimental evidence was reported by the BESIII collaboration [28,29]. In fact, for equal masses and lacking an ideal decay channel, the observation of the $a_0(980)$ - $f_0(980)$ mixing is very

challenging. But, the case of the $a_0(1710)$ - $f_0(1710)$ mixing is different, which can potentially be observed in the experiments, and studying this mixing effect is the motivation of the present work. Furthermore, it should be mentioned that the mixing dynamic of the a_0 - f_0 states is different from the case of the η - η' mixing, which comes from the spontaneous breaking of the $SU(3)$ chiral symmetry; whereas, the mixing of the a_0 - f_0 states arises from the isospin violation and is related to the mass difference between the neutral and charge kaons in the $K\bar{K}$ loops, which is a consequence of the molecular description of the a_0 - f_0 states.

In the molecular picture, the interaction of $K^* \bar{K}^*$ is analogous to that of $K\bar{K}$, where one would expect that similar resonances emerge. The $f_0(1710)$ state was first observed about 40 years ago [30,31]. At first, it was interpreted as a normal light scalar meson in the conventional quark model [4,32], and an isovector partner state of 1.78 GeV was predicted. Furthermore, the $f_0(1710)$ was also regarded as a candidate of the scalar glueball [33–41]. But, as pointed out in Refs. [42,43], the $f_0(1710)$ may contain large $s\bar{s}$ quark components because it mainly decays to the $K\bar{K}$ and $\eta\eta$ channels. Thus, from the coupled channel interaction's point of view, it was considered as a molecular state of $K^* \bar{K}^*$ in Ref. [44], where an isovector partner a_0 state around 1.78 GeV was predicted. A similar prediction from the $K^* \bar{K}^*$ interactions also can be found in Refs. [45,46]. The possibility that $f_0(1710)$, being a molecular state, was dynamically generated from the

*Contact author: 212201014@csu.edu.cn

†Contact author: xiaochw@gxnu.edu.cn

Published by the American Physical Society under the terms of the [Creative Commons Attribution 4.0 International license](https://creativecommons.org/licenses/by/4.0/). Further distribution of this work must maintain attribution to the author(s) and the published article's title, journal citation, and DOI. Funded by SCOAP³.

vector-vector coupled channel interactions was discussed in Refs. [47–54].

Therefore, searching for $f_0(1710)$'s isovector partner is crucial to pin down whether it is a glueball or a molecular state. Until 2021, a new state $a_0(1700)$ in the $\pi\eta$ invariant mass spectrum was observed in the $\eta_c \rightarrow \eta\pi^+\pi^-$ decay by the *BABAR* collaboration [55], of which the mass and the width were given by (1.704 ± 0.005) and (0.110 ± 0.019) GeV, respectively. Moreover, the $f_0(1710)$ was also observed in the decays $\eta_c \rightarrow \eta'K^+K^-(\pi^+\pi^-)$ [55], which was consistent with the observation of the radiative decays $\Upsilon \rightarrow \gamma K^+K^-(\pi^+\pi^-)$ [56]. Furthermore, the decay $D_s^+ \rightarrow \pi^+K_S^0K_S^0$ was investigated by the BESIII collaboration [57], where a resonance structure in the energy region around 1.710 GeV was observed in the $K_S^0K_S^0$ mass distribution, with mass $M_{S(1710)} = (1.723 \pm 0.011)$ GeV and width $\Gamma_{S(1710)} = (0.140 \pm 0.015)$ GeV. Note that, due to the $a_0(1710)$ and $f_0(1710)$ having identical quantum number $J^{PC} = 0^{++}$ and their masses are assumed to be identical in Ref. [57], they were not distinguished and assigned as $S(1710)$ in this reference, which is in analogy to $S(980)$ for the states $a_0(980)$ and $f_0(980)$. In fact, the $S(1710)$ and $S(980)$ were the ‘‘mixing’’ signals in the decay $D_s^+ \rightarrow \pi^+K_S^0K_S^0$. Indeed, the admixture signal of $S(980)$ was also observed in the decay $D_s^+ \rightarrow K^+K^-\pi^+$ [58,59], where the $f_0(1710)$ was also seen. Because of the overlap of $a_0(1710)^0$ and $f_0(1710)$, the BESIII collaboration continued to measure the related decay $D_s^+ \rightarrow K_S^0K^+\pi^0$ [60], and observed a resonance $a_0(1710)^+$ in the $K_S^0K^+$ invariant mass spectrum, $M_{a_0(1710)} = (1.817 \pm 0.022)$ GeV and $\Gamma_{a_0(1710)} = (0.097 \pm 0.027)$ GeV, which was called the $a_0(1817)$ state in the literature existing then.¹ Indeed, the measured mass of a state may be different when it is found in different decay processes. In most cases, one can depend on its decay modes to assign a state, such as the $f_0(1770)$ state [61] found by the BES collaboration [62]. The mass of the $f_0(1770)$ is close to the $f_0(1710)$ with similar width, of which the nature was discussed in Refs. [63,64]. The $f_0(1710)$ mainly decay into the channel $K\bar{K}$, whereas, the dominant decay channel of the $f_0(1770)$ is $\pi\pi$.

As suggested in Ref. [65], the finding of Ref. [60] should be properly named as $a_0(1817)$, which was arranged in the same Regge trajectory with the $a_0(980)$; whereas, it was assigned as $a_0(1710)$ in Ref. [66] from the coupled channel interaction of $K^*\bar{K}^*$. Using the coupled channel for the final state interaction, the decay $D_s^+ \rightarrow K_S^0K^+\pi^0$ was investigated in Refs. [67,68], where the new state of Ref. [60] was assumed as the $a_0(1710)$. Note that a combined fit for the invariant mass distributions was performed in Ref. [68],

where a pole $(1.7936 + 0.0094i)$ GeV was found for the $a_0(1710)$. Also applying the final state interaction approach, the decay $D_s^+ \rightarrow \pi^+K_S^0K_S^0$ was studied in Refs. [69,70], $\eta_c \rightarrow \bar{K}^0K^+\pi^-$ in Ref. [71], and $J/\psi \rightarrow \bar{K}^0K^+\rho^-$ in Ref. [72]. With the MIT bag model, it was found in Ref. [73] that the a_0 strongly couples to the vector channels, such as $K^*\bar{K}^*$, $\rho\phi$, and so on, depending on the mass of the a_0 ; thus, these vector channels should be detected to understand the nature of the new a_0 . Furthermore, more comments on the $a_0(1710)$ can be found in Ref. [74] with some proposals for future experiments. Thus, in the present work, to understand more about the nature of $a_0(1710)$, we investigate the decay $D_s^+ \rightarrow \pi^+K_S^0K_S^0$ with the final state interaction formalism. Note that, in this work, we use eleven coupled channels to dynamically reproduce the $a_0(1710)$ and also make a combined fit for the invariant mass distributions, where the mixing effect is found; see our results later. This is different when compared to the works of [69,70], where the Breit-Wigner amplitude was used for the $a_0(1710)$ state.

The rest of the paper is organized as follows. In Sec. II, we introduce the final state interaction formalism for the $D_s^+ \rightarrow K_S^0K_S^0\pi^+$ decay in detail. The results of combined fits for the $K_S^0K_S^0$ and $K_S^0\pi^+$ invariant mass distributions, and the branching ratios of different intermediate resonances are presented in Sec. III. Then, a short summary is made in Sec. IV.

II. THEORETICAL FRAMEWORK

In this work, we investigate the three-body weak decay $D_s^+ \rightarrow K_S^0K_S^0\pi^+$. First, we consider the dynamics at the quark level with the external and internal emission mechanisms of the W boson [75–77]. Then, at the hadron level, we take into account the final state interactions in the S wave, and the contribution from the vector meson resonance produced in the P wave.

For the $D_s^+ \rightarrow K_S^0K_S^0\pi^+$ decay, we only consider the contributions of the weak decay topology from the W -external and W -internal emission mechanisms, which are the dominant ones. The related Feynman diagrams are shown in Figs. 1 and 2. In Fig. 1, the c quark coming from D_s^+ decays into the W^+ boson and the s quark, and then the W^+ boson decays into a $u\bar{d}$ quark pair, while the \bar{s} quark remains unchanged. There are two possible hadronization processes. First, the $u\bar{d}$ quark pair forms a π^+ or ρ^+ meson directly, while the $s\bar{s}$ quark pair decays into two mesons via hadronization with $q\bar{q} = u\bar{u} + d\bar{d} + s\bar{s}$ produced from the vacuum. Second, the $s\bar{s}$ quark pair goes into a ϕ or η meson, while the $u\bar{d}$ quark pair created by the W^+ boson undergoes the hadronization. The corresponding processes for these hadronizations can be written as

¹In the updated online version of Particle Data Group (PDG) [61], it was named $a_0(1710)$.

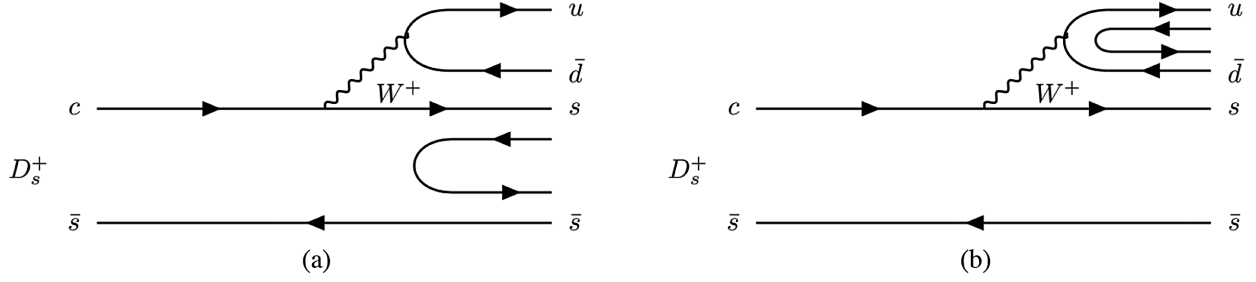


FIG. 1. W -external emission mechanism for the $D_s^+ \rightarrow K_S^0 K_S^0 \pi^+$ decay. (a) The $s\bar{s}$ quark pair hadronizes into final mesons. (b) The $u\bar{d}$ quark pair hadronizes into final mesons.

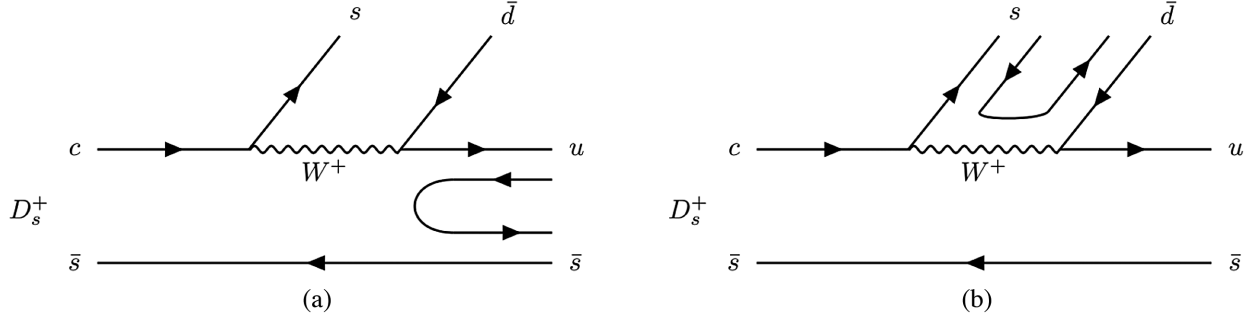


FIG. 2. W -internal emission mechanism for the $D_s^+ \rightarrow K_S^0 K_S^0 \pi^+$ decay. (a) The $u\bar{s}$ quark pair hadronizes into final mesons. (b) The $s\bar{d}$ quark pair hadronizes into final mesons.

$$\begin{aligned}
 |H^{(1a)}\rangle &= V_P^{(1a)} V_{cs} V_{ud} (u\bar{d} \rightarrow \pi^+) |s(\bar{u}u + \bar{d}d + \bar{s}s)\bar{s}\rangle \\
 &\quad + V_P^{*(1a)} V_{cs} V_{ud} (u\bar{d} \rightarrow \rho^+) |s(\bar{u}u + \bar{d}d + \bar{s}s)\bar{s}\rangle \\
 &= V_P^{(1a)} V_{cs} V_{ud} (\pi^+) (M \cdot M)_{33} \\
 &\quad + V_P^{*(1a)} V_{cs} V_{ud} (\rho^+) (M \cdot M)_{33}, \tag{1}
 \end{aligned}$$

$$\begin{aligned}
 |H^{(1b)}\rangle &= V_P^{(1b)} V_{cs} V_{ud} \left(s\bar{s} \rightarrow -\frac{2}{\sqrt{6}}\eta \right) |u(\bar{u}u + \bar{d}d + \bar{s}s)\bar{d}\rangle \\
 &\quad + V_P^{*(1b)} V_{cs} V_{ud} (s\bar{s} \rightarrow \phi) |u(\bar{u}u + \bar{d}d + \bar{s}s)\bar{d}\rangle \\
 &= V_P^{(1b)} V_{cs} V_{ud} \left(-\frac{2}{\sqrt{6}}\eta \right) (M \cdot M)_{12} \\
 &\quad + V_P^{*(1b)} V_{cs} V_{ud} (\phi) (M \cdot M)_{12}, \tag{2}
 \end{aligned}$$

where the factors $V_P^{(1a)}$, $V_P^{*(1a)}$, $V_P^{(1b)}$, and $V_P^{*(1b)}$ are the weak interaction strengths of the production vertices to generate π^+ , ρ^+ , η , and ϕ mesons, respectively [78,79]. These factors contain all dynamical information and can be regarded as the constants determined by the experimental data fits. The factor $-\frac{2}{\sqrt{6}}$ is due to the flavor component $s\bar{s}$ of η meson, where we take $\eta = \eta_8$.² The factors V_{cs} and

V_{ud} are the elements from the Cabibbo-Kobayashi-Maskawa (CKM) matrix. The elements of $q\bar{q}$ quark pairs can form a matrix M in SU(3), which is defined as

$$M = \begin{pmatrix} u\bar{u} & u\bar{d} & u\bar{s} \\ d\bar{u} & d\bar{d} & d\bar{s} \\ s\bar{u} & s\bar{d} & s\bar{s} \end{pmatrix}. \tag{3}$$

Similarly, the case of the W -internal emission is shown in Fig. 2, which also contains two possible hadronization processes. First, the $s\bar{d}$ quark pair goes into a \bar{K}^0 or \bar{K}^{*0} meson; the $u\bar{s}$ quark pair hadronizes with the $q\bar{q}$ quark pairs produced from the vacuum. Second, the $u\bar{s}$ quark pair forms a K^+ or K^{*+} meson, while the $s\bar{d}$ quark pair hadronizes into two final states with the $q\bar{q}$ quark pairs produced from the vacuum. Then, these processes can be written as

$$\begin{aligned}
 |H^{(2a)}\rangle &= V_P^{(2a)} V_{cs} V_{ud} (s\bar{d} \rightarrow \bar{K}^0) |u(\bar{u}u + \bar{d}d + \bar{s}s)\bar{s}\rangle \\
 &\quad + V_P^{*(2a)} V_{cs} V_{ud} (s\bar{d} \rightarrow \bar{K}^{*0}) |u(\bar{u}u + \bar{d}d + \bar{s}s)\bar{s}\rangle \\
 &= V_P^{(2a)} V_{cs} V_{ud} (\bar{K}^0) (M \cdot M)_{13} \\
 &\quad + V_P^{*(2a)} V_{cs} V_{ud} (\bar{K}^{*0}) (M \cdot M)_{13}, \tag{4}
 \end{aligned}$$

²If one considers the η - η' mixing, the matrix P of Eq. (6) will be different, see Ref. [80].

$$\begin{aligned}
 |H^{(2b)}\rangle &= V_P^{(2b)} V_{cs} V_{ud} (u\bar{s} \rightarrow K^+) |s(\bar{u}u + \bar{d}d + \bar{s}s)\bar{d}\rangle \\
 &\quad + V_P^{*(2b)} V_{cs} V_{ud} (u\bar{s} \rightarrow K^{*+}) |s(\bar{u}u + \bar{d}d + \bar{s}s)\bar{d}\rangle \\
 &= V_P^{(2b)} V_{cs} V_{ud} (K^+) (M \cdot M)_{32} \\
 &\quad + V_P^{*(2b)} V_{cs} V_{ud} (K^{*+}) (M \cdot M)_{32}, \quad (5)
 \end{aligned}$$

where the factors $V_P^{(2a)}$, $V_P^{*(2a)}$, $V_P^{(2b)}$, and $V_P^{*(2b)}$ are the production vertices to generate \bar{K}^0 , \bar{K}^{*0} , K^+ , and K^{*+} mesons, respectively. Subsequently, after the hadronization, the matrix M at the quark level can be transferred to the hadron level form in the terms of the pseudoscalar (P) or vector (V) mesons, rewritten as

$$P = \begin{pmatrix} \frac{1}{\sqrt{2}}\pi^0 + \frac{1}{\sqrt{6}}\eta & \pi^+ & K^+ \\ \pi^- & -\frac{1}{\sqrt{2}}\pi^0 + \frac{1}{\sqrt{6}}\eta & K^0 \\ K^- & \bar{K}^0 & -\frac{2}{\sqrt{6}}\eta \end{pmatrix}, \quad (6)$$

$$V = \begin{pmatrix} \frac{1}{\sqrt{2}}\rho^0 + \frac{1}{\sqrt{2}}\omega & \rho^+ & K^{*+} \\ \rho^- & -\frac{1}{\sqrt{2}}\rho^0 + \frac{1}{\sqrt{2}}\omega & K^{*0} \\ K^{*-} & \bar{K}^{*0} & \phi \end{pmatrix}, \quad (7)$$

where we take $\eta \equiv \eta_8$ as done in Refs. [81,82]. It should be mentioned that the component $(M \cdot M)_{ij}$ has four situations with two matrices of physical meson, such as $(P \cdot P)_{ij}$, $(V \cdot V)_{ij}$, $(V \cdot P)_{ij}$, and $(P \cdot V)_{ij}$. Then, one can rewrite the hadronization processes mentioned above, where the explicit formulas are given by

$$\begin{aligned}
 |H^{(1a)}\rangle &= V_{cs} V_{ud} V_P^{(1a)} \left(\pi^+ K^+ K^- + \pi^+ K^0 \bar{K}^0 + \frac{2}{3} \eta \eta \pi^+ \right) \\
 &\quad + V_{cs} V_{ud} V_P^{(1a)} \left(\pi^+ K^{*+} K^{*-} + \pi^+ K^{*0} \bar{K}^{*0} \right) \\
 &\quad + \phi \phi \pi^+, \quad (8)
 \end{aligned}$$

$$\begin{aligned}
 |H^{(1b)}\rangle &= V_{cs} V_{ud} V_P^{(1b)} \left(-\frac{2}{3} \eta \eta \pi^+ \right) \\
 &\quad + V_{cs} V_{ud} \hat{V}_P^{*(1b)} \left(-\frac{1}{\sqrt{2}} \pi^+ \rho^0 \phi + \frac{1}{\sqrt{2}} \pi^+ \omega \phi \right) \\
 &\quad + V_{cs} V_{ud} \bar{V}_P^{*(1b)} \left(\frac{1}{\sqrt{2}} \pi^+ \rho^0 \phi + \frac{1}{\sqrt{2}} \pi^+ \omega \phi \right), \quad (9)
 \end{aligned}$$

$$\begin{aligned}
 |H^{(2a)}\rangle &= V_{cs} V_{ud} V_P^{(2a)} (\pi^+ K^0 \bar{K}^0) \\
 &\quad + V_{cs} V_{ud} \hat{V}_P^{*(2a)} (\pi^+ K^{*0} \bar{K}^{*0}), \quad (10)
 \end{aligned}$$

$$\begin{aligned}
 |H^{(2b)}\rangle &= V_{cs} V_{ud} V_P^{(2b)} (\pi^+ K^+ K^-) \\
 &\quad + V_{cs} V_{ud} \bar{V}_P^{*(2b)} (\pi^+ K^{*+} K^{*-}), \quad (11)
 \end{aligned}$$

where we only keep the terms that contribute to the final states $K_S^0 K_S^0 \pi^+$. Besides, in order to distinguish the contribution from the different terms of $(M \cdot M)_{ij}$, we adopt $V_P^{(1a/1b/2a/2b)}$, $V_P^{*(1a/1b/2a/2b)}$, $\bar{V}_P^{*(1a/1b/2a/2b)}$, and $\hat{V}_P^{*(1a/1b/2a/2b)}$ to represent the $(P \cdot P)_{ij}$, $(V \cdot V)_{ij}$, $(V \cdot P)_{ij}$, and $(P \cdot V)_{ij}$, respectively, where the superscripts 1a/1b/2a/2b denote the contributions of the corresponding subfigures of Figs. 1 and 2, respectively. Then we obtain the total contributions in the S wave,

$$\begin{aligned}
 |H\rangle &= |H^{(1a)}\rangle + |H^{(1b)}\rangle + |H^{(2a)}\rangle + |H^{(2b)}\rangle \\
 &= V_{cs} V_{ud} \left(V_P^{(1a)} + V_P^{(2b)} \right) \pi^+ K^+ K^- + V_{cs} V_{ud} \left(V_P^{(1a)} + V_P^{(2a)} \right) \pi^+ K^0 \bar{K}^0 \\
 &\quad + \frac{2}{3} V_{cs} V_{ud} \left(V_P^{(1a)} - V_P^{(1b)} \right) \pi^+ \eta \eta + V_{cs} V_{ud} \left(V_P^{(1a)} + \bar{V}_P^{*(2b)} \right) \pi^+ K^{*+} K^{*-} \\
 &\quad + V_{cs} V_{ud} \left(V_P^{(1a)} + \hat{V}_P^{*(2a)} \right) \pi^+ K^{*0} \bar{K}^{*0} + V_{cs} V_{ud} V_P^{(1a)} \pi^+ \phi \phi \\
 &\quad + \frac{1}{\sqrt{2}} V_{cs} V_{ud} \left(\hat{V}_P^{*(1b)} + \bar{V}_P^{*(1b)} \right) \pi^+ \omega \phi + \frac{1}{\sqrt{2}} V_{cs} V_{ud} \left(-\hat{V}_P^{*(1b)} + \bar{V}_P^{*(1b)} \right) \pi^+ \rho^0 \phi \\
 &= C_1 \pi^+ K^+ K^- + C_2 \pi^+ K^0 \bar{K}^0 + \frac{2}{3} C_3 \pi^+ \eta \eta + C_4 \pi^+ K^{*+} K^{*-} + C_5 \pi^+ K^{*0} \bar{K}^{*0} \\
 &\quad + C_6 \pi^+ \phi \phi + \frac{1}{\sqrt{2}} C_7 \pi^+ \omega \phi + \frac{1}{\sqrt{2}} C_8 \pi^+ \rho^0 \phi, \quad (12)
 \end{aligned}$$

where the factors C_1 , C_2 , C_3 , C_4 , C_5 , C_6 , C_7 , and C_8 are defined as $C_1 = V_{cs} V_{ud} \left(V_P^{(1a)} + V_P^{(2b)} \right)$, $C_2 = V_{cs} V_{ud} \left(V_P^{(1a)} + V_P^{(2a)} \right)$, $C_3 = V_{cs} V_{ud} \left(V_P^{(1a)} - V_P^{(1b)} \right)$, $C_4 = V_{cs} V_{ud} \left(V_P^{(1a)} + \bar{V}_P^{*(2b)} \right)$, $C_5 = V_{cs} V_{ud} \left(V_P^{(1a)} + \hat{V}_P^{*(2a)} \right)$, $C_6 = V_{cs} V_{ud} \left(V_P^{(1a)} \right)$, $C_7 = V_{cs} V_{ud} \left(\hat{V}_P^{*(1b)} + \bar{V}_P^{*(1b)} \right)$, and $C_8 = V_{cs} V_{ud} \left(-\hat{V}_P^{*(1b)} + \bar{V}_P^{*(1b)} \right)$. Note that the elements of

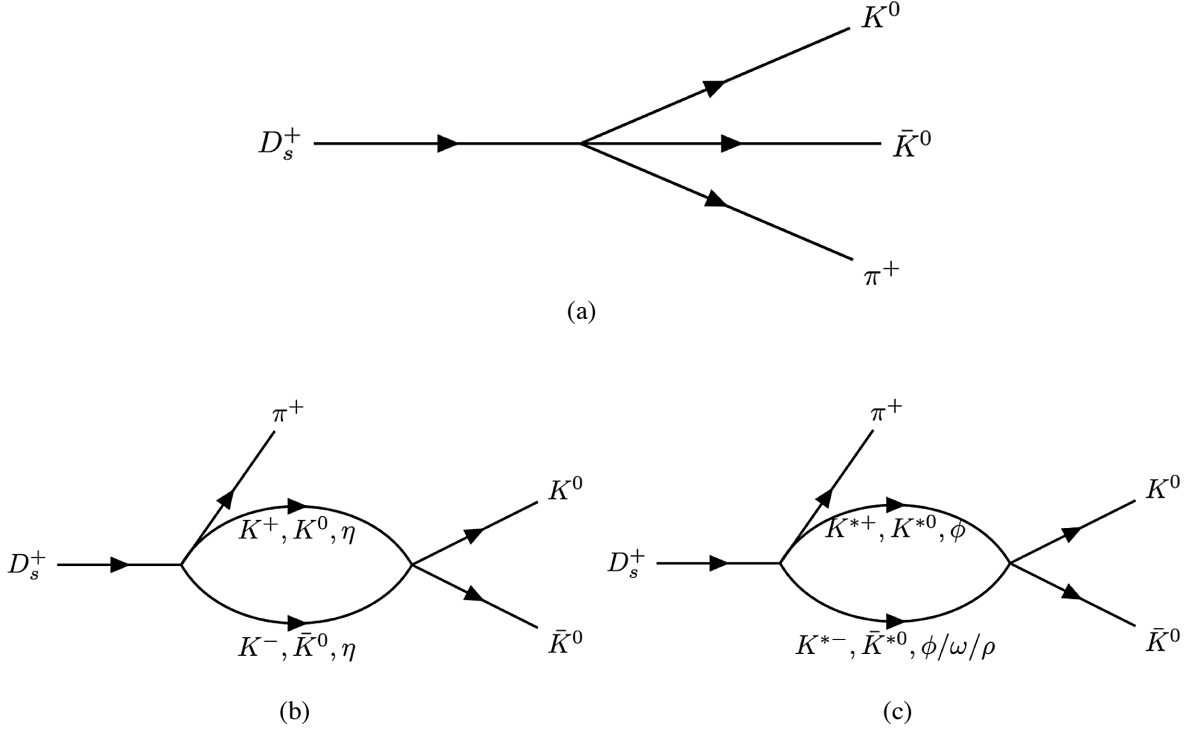


FIG. 3. Diagrammatic representations of the $D_s^+ \rightarrow K_S^0 K_S^0 \pi^+$ decay. (a) Tree-level diagram. (b) Rescattering of $K^+ K^-$, $K^0 \bar{K}^0$, and $\eta\eta$. (c) Rescattering of $K^{*+} K^{*-}$, $K^{*0} \bar{K}^{*0}$, $\phi\phi$, $\phi\omega$, and $\phi\rho$.

the CKM matrix and the vertex factors of weak decay are absorbed in these factors C_i . In our formalism, these parameters are taken as free constants, which also include a global normalization factor to match the events of the experimental data when we determine them by fitting the invariant mass distributions later. From Eq. (12), one can see that the final states $K_S^0 K_S^0 \pi^+$ can produce directly in the hadronization processes, while the remaining part can get these final states via rescattering procedures, which are shown in Fig. 3.

Therefore, under the dominant W -external and W -internal emission mechanisms, the amplitude of $D_s^+ \rightarrow K_S^0 K_S^0 \pi^+$ decay process in the S wave can be written as

$$\begin{aligned}
 t(M_{12})|_{K^0 \bar{K}^0 \pi^+} &= C_1 G_{K^+ K^-}(M_{12}) T_{K^+ K^- \rightarrow K^0 \bar{K}^0}(M_{12}) + C_2 + C_2 G_{K^0 \bar{K}^0}(M_{12}) T_{K^0 \bar{K}^0 \rightarrow K^0 \bar{K}^0}(M_{12}) \\
 &+ \frac{2}{3} C_3 G_{\eta\eta}(M_{12}) T_{\eta\eta \rightarrow K^0 \bar{K}^0}(M_{12}) + C_4 G_{K^{*+} K^{*-}}(M_{12}) T_{K^{*+} K^{*-} \rightarrow K^0 \bar{K}^0}(M_{12}) \\
 &+ C_5 G_{K^{*0} \bar{K}^{*0}}(M_{12}) T_{K^{*0} \bar{K}^{*0} \rightarrow K^0 \bar{K}^0}(M_{12}) + C_6 G_{\phi\phi}(M_{12}) T_{\phi\phi \rightarrow K^0 \bar{K}^0}(M_{12}) \\
 &+ \frac{1}{\sqrt{2}} C_7 G_{\omega\phi}(M_{12}) T_{\omega\phi \rightarrow K^0 \bar{K}^0}(M_{12}) + \frac{1}{\sqrt{2}} C_8 G_{\rho^0\phi}(M_{12}) T_{\rho^0\phi \rightarrow K^0 \bar{K}^0}(M_{12}), \tag{13}
 \end{aligned}$$

where M_{ij} is the energy of two particles in the center-of-mass (c.m.) frame, and the subscripts $i, j = 1, 2, 3$ denote three final states of K^0 , \bar{K}^0 , and π^+ , respectively. Then, we take $|K_S^0\rangle = \frac{1}{\sqrt{2}}(|K^0\rangle - |\bar{K}^0\rangle)$ into account [69] and change the final states from K^0 and \bar{K}^0 to K_S^0 , and thus, Eq. (13) can be revised into

$$\begin{aligned}
 t(M_{12})|_{K_S^0 K_S^0 \pi^+} &= -\frac{1}{2} C_1 G_{K^+ K^-}(M_{12}) T_{K^+ K^- \rightarrow K^0 \bar{K}^0}(M_{12}) - \frac{1}{2} C_2 - \frac{1}{2} C_2 G_{K^0 \bar{K}^0}(M_{12}) T_{K^0 \bar{K}^0 \rightarrow K^0 \bar{K}^0}(M_{12}) \\
 &- \frac{1}{3} C_3 G_{\eta\eta}(M_{12}) T_{\eta\eta \rightarrow K^0 \bar{K}^0}(M_{12}) - \frac{1}{2} C_4 G_{K^{*+} K^{*-}}(M_{12}) T_{K^{*+} K^{*-} \rightarrow K^0 \bar{K}^0}(M_{12}) \\
 &- \frac{1}{2} C_5 G_{K^{*0} \bar{K}^{*0}}(M_{12}) T_{K^{*0} \bar{K}^{*0} \rightarrow K^0 \bar{K}^0}(M_{12}) - \frac{1}{2} C_6 G_{\phi\phi}(M_{12}) T_{\phi\phi \rightarrow K^0 \bar{K}^0}(M_{12}) \\
 &- \frac{1}{2\sqrt{2}} C_7 G_{\omega\phi}(M_{12}) T_{\omega\phi \rightarrow K^0 \bar{K}^0}(M_{12}) - \frac{1}{2\sqrt{2}} C_8 G_{\rho^0\phi}(M_{12}) T_{\rho^0\phi \rightarrow K^0 \bar{K}^0}(M_{12}), \tag{14}
 \end{aligned}$$

where $G_{PP'(VV')}$ and $T_{PP'(VV')\rightarrow PP'}$ are the loop functions and the two-body scattering amplitudes, respectively; see the detail below.

The matrix G is diagonal, which is made up of the meson-meson loop function. The explicit form of the loop function with the dimensional regularization is given by [83–87]

$$G_{PP'}(M_{\text{inv}}) = \frac{1}{16\pi^2} \left\{ a_\mu(\mu) + \ln \frac{m_2^2}{\mu^2} + \frac{m_2^2 - m_1^2 + M_{\text{inv}}^2}{2M_{\text{inv}}^2} \ln \frac{m_2^2}{m_1^2} + \frac{q_{\text{cm}}(M_{\text{inv}})}{M_{\text{inv}}} [\ln (M_{\text{inv}}^2 - (m_2^2 - m_1^2) + 2q_{\text{cm}}(M_{\text{inv}})M_{\text{inv}}) + \ln (M_{\text{inv}}^2 + (m_2^2 - m_1^2) + 2q_{\text{cm}}(M_{\text{inv}})M_{\text{inv}}) - \ln (-M_{\text{inv}}^2 - (m_2^2 - m_1^2) + 2q_{\text{cm}}(M_{\text{inv}})M_{\text{inv}}) - \ln (-M_{\text{inv}}^2 + (m_2^2 - m_1^2) + 2q_{\text{cm}}(M_{\text{inv}})M_{\text{inv}})] \right\}, \quad (15)$$

where m_1 and m_2 are the masses of two intermediate particles in the loop, M_{inv} is the invariant mass of two mesons in the system, and μ is the regularization scale, of which the value will be determined by fitting experimental data in Sec. III. Besides, $a(\mu)$ is the subtraction constant, of which the value can be evaluated by [83,88,89]

$$a(\mu) = -2 \ln \left(1 + \sqrt{1 + \frac{m_1^2}{\mu^2}} \right) + \dots, \quad (16)$$

where m_1 is the mass of a larger-mass meson in the corresponding channels, while the ellipses indicate the ignored higher order terms in the nonrelativistic expansion [90]. Furthermore, $q_{\text{cm}}(M_{\text{inv}})$ is the three-momentum of the particles in the c.m. frame,

$$q_{\text{cm}}(M_{\text{inv}}) = \frac{\lambda^{1/2}(M_{\text{inv}}^2, m_1^2, m_2^2)}{2M_{\text{inv}}}, \quad (17)$$

with the usual Källén triangle function $\lambda(a, b, c) = a^2 + b^2 + c^2 - 2(ab + ac + bc)$.

Moreover, the two-body scattering amplitude in Eq. (14) can be calculated by the coupled channel Bethe-Salpeter equation [14,91],

$$T = [1 - VG]^{-1}V, \quad (18)$$

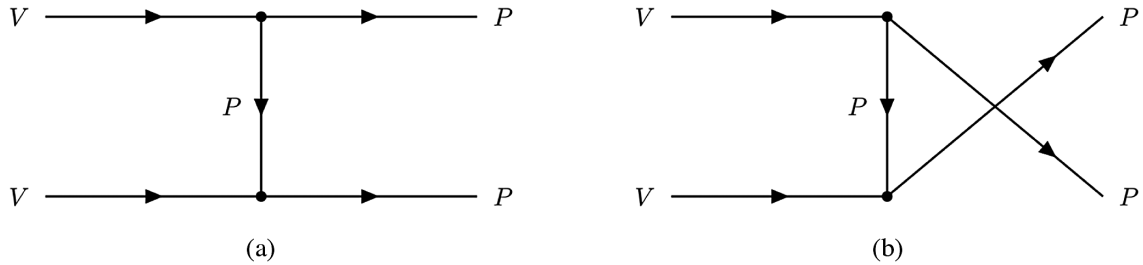


FIG. 4. Feynman diagrams of (a) the t channel and (b) the u channel.

where the matrix G is constructed by the loop functions, the element of which is given by Eq. (15), and the matrix V is made of the interaction potential for each coupled channel. For isospin $I = 1$ sector, we consider six channels: (1) $K^* \bar{K}^*$, (2) $\rho\omega$, (3) $\rho\phi$, (4) $\rho\rho$, (5) $K\bar{K}$, and (6) $\pi\eta$. For isospin $I = 0$ sector, we consider eight channels: (1) $K^* \bar{K}^*$, (2) $\rho\rho$, (3) $\omega\omega$, (4) $\omega\phi$, (5) $\phi\phi$, (6) $\pi\pi$, (7) $K\bar{K}$, and (8) $\eta\eta$. Among them, the potentials $V_{VV\rightarrow VV}$ are taken from Ref. [44], which considered the tree-level transition of four-vector-contact diagrams and the t/u -channel vector meson-exchange terms. The potentials $V_{PP\rightarrow PP}$ are taken from Refs. [14,81,88,92,93], which only include the tree-level contributions. Besides, the potentials $V_{VV\rightarrow PP}$ are calculated as done in Ref. [66], where the Feynman diagrams of t and u channels are considered, as shown in Fig. 4. The Lagrangian for the VPP vertex is given by [94,95]

$$\mathcal{L}_{VPP} = -ig \langle V_\mu [P, \partial^\mu P] \rangle, \quad (19)$$

where the symbol $\langle \dots \rangle$ stands for the trace in color space, $g = M_V/(2f_\pi)$ with $M_V = 0.84566$ GeV, which is the averaged vector-meson mass, and $f_\pi = 0.093$ GeV is pion decay constant, which is taken from Refs. [14,66]. Then, some parts of the potentials of $V_{VV\rightarrow PP}$ are given by (for simplicity not listing them all)

$$\begin{aligned}
 V_{K^{*+}K^{*-} \rightarrow K^0\bar{K}^0} &= -\frac{4}{t-m_\pi^2} g^2 \epsilon_{1\mu} k_3^\mu \epsilon_{2\nu} k_4^\nu, \\
 V_{K^{*0}\bar{K}^{*0} \rightarrow K^0\bar{K}^0} &= -2 \left(\frac{3}{t-m_\eta^2} + \frac{1}{t-m_\pi^2} \right) g^2 \epsilon_{1\mu} k_3^\mu \epsilon_{2\nu} k_4^\nu, \\
 V_{\phi\phi \rightarrow K^0\bar{K}^0} &= -4g^2 \left(\frac{1}{t-m_K^2} \epsilon_{1\mu} k_3^\mu \epsilon_{2\nu} k_4^\nu + \frac{1}{u-m_K^2} \epsilon_{1\mu} k_4^\mu \epsilon_{2\nu} k_3^\nu \right), \\
 V_{\omega\phi \rightarrow K^0\bar{K}^0} &= 2\sqrt{2}g^2 \left(\frac{1}{t-m_K^2} \epsilon_{1\mu} k_3^\mu \epsilon_{2\nu} k_4^\nu + \frac{1}{u-m_K^2} \epsilon_{1\mu} k_4^\mu \epsilon_{2\nu} k_3^\nu \right), \\
 V_{\rho\phi \rightarrow K^0\bar{K}^0} &= -2\sqrt{2} \left(\frac{1}{t-m_K^2} g^2 \epsilon_{1\mu} k_3^\mu \epsilon_{2\nu} k_4^\nu + \frac{1}{u-m_K^2} g^2 \epsilon_{1\mu} k_4^\mu \epsilon_{2\nu} k_3^\nu \right),
 \end{aligned} \tag{20}$$

where $t = (k_1 - k_3)^2$ and $u = (k_1 - k_4)^2$, ϵ_i is the polarization vector, and k_i is the four-momentum of the corresponding particles, of which the subscript i ($i = 1, 2, 3, 4$) denotes the particles in scattering process $V(1)V(2) \rightarrow P(3)P(4)$. It is worth mentioning that, as done in Refs. [46,96], we also introduce a monopole form factor for each VPP vertex of the exchanged pseudoscalar meson, of which the explicit expression is given by

$$F = \frac{\Lambda^2 - m_{ex}^2}{\Lambda^2 - q^2}, \tag{21}$$

where m_{ex} is the mass of the exchanged pseudoscalar meson, q is the transferred momentum, and the value of parameter Λ is empirically chosen as 1.0 GeV. After performing the partial wave projection, we can obtain the S -wave potentials $V_{VV \rightarrow PP}$, where we take proper approximation for them due to the problem of the discontinuity and singularity in the left-hand cut. Note that these nondiagonal potentials from the transitions $V_{VV \rightarrow PP}$ are in fact weak compared to the diagonal ones from the vector meson exchanges. Thus, for simplicity, one can safely ignore the suppressed vector meson exchange in the transitions $V_{VV \rightarrow PP}$, which was taken into account in the work of [66].

Furthermore, we also consider the contribution of the vector resonance generated in the P wave. As discussed above, the vector meson both with the W -external and

W -internal emission mechanisms can be produced directly. Thus, the vector meson coming from hadronization, such as $K^*(892)^+$, which is not generated in the meson-meson rescattering process, would also decay to the final states that we are looking for. The production mechanism is depicted in Fig. 5, and the relativistic amplitude for the decay $D_s^+ \rightarrow K_S^0 K^*(892)^+ \rightarrow K_S^0 K_S^0 \pi^+$ can be written as [82,97]

$$\begin{aligned}
 &t_{K^*(892)^+}(M_{12}, M_{23}) \\
 &= \frac{\mathcal{D} e^{i\alpha_{K^*(892)^+}}}{M_{23}^2 - M_{K^*(892)^+}^2 + iM_{K^*(892)^+}\Gamma_{K^*(892)^+}} \\
 &\times \left[\frac{(m_{D_s^+}^2 - m_{K_S^0}^2)(m_{K_S^0}^2 - m_{\pi^+}^2)}{M_{K^*(892)^+}^2} - M_{12}^2 + M_{13}^2 \right],
 \end{aligned} \tag{22}$$

where \mathcal{D} and $\alpha_{K^*(892)^+}$ are the normalization constant and the phase, respectively, which can be determined by fitting the experimental data. The mass and width of intermediate $K^*(892)^+$ are taken from the PDG [61], of which the values are $M_{K^*(892)^+} = 0.89167$ GeV and $\Gamma_{K^*(892)^+} = 0.0514$ GeV. Although there are three s_{ij} variables, only two of them are independent, which fulfill the constraint condition,

$$M_{12}^2 + M_{13}^2 + M_{23}^2 = m_{D_s^+}^2 + m_{K_S^0}^2 + m_{K_S^0}^2 + m_{\pi^+}^2. \tag{23}$$

Finally, the double differential width distribution for the three-body decay $D_s^+ \rightarrow K_S^0 K_S^0 \pi^+$ can be calculated by [61]

$$\frac{d^2\Gamma}{dM_{12}dM_{23}} = \frac{1}{(2\pi)^3} \frac{M_{12}M_{23}}{8m_{D_s^+}^3} \frac{1}{2} |\mathcal{M}|^2, \tag{24}$$

where the factor $1/2$ comes from the identical particle K_S^0 in the final states, and \mathcal{M} is the total amplitude of the decay $D_s^+ \rightarrow K_S^0 K_S^0 \pi^+$. From the discussions above, the total amplitude of \mathcal{M} is written as

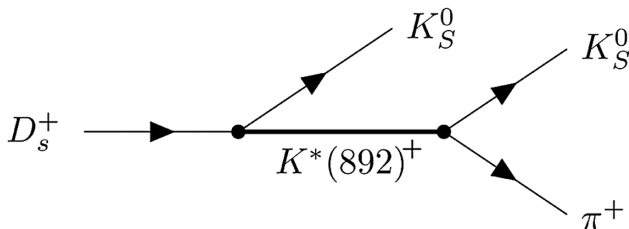


FIG. 5. Mechanism of $D_s^+ \rightarrow K_S^0 K_S^0 \pi^+$ decay via the intermediate state $K^*(892)^+$.

TABLE I. Values of the parameters from the fit.

Parameters	μ	C_1	C_2	C_3
Fit	0.648 ± 0.01 GeV	8640.90 ± 1115.80	2980.71 ± 638.37	-1902.86 ± 293.27
Parameters	C_4	C_5	C_6	C_7
Fit	56906.35 ± 10869.67	-13433.15 ± 5017.76	-58284.22 ± 7319.04	102835.76 ± 23333.56
Parameters	C_8	D	$\alpha_{K^*(892)^+}$	$\chi^2/\text{d.o.f.}$
Fit	202807.71 ± 30750.45	54.8 ± 2.0	0.0024 ± 4.30	2.55

$$\mathcal{M} = t(M_{12})|_{K_S^0 K_S^0 \pi^+} + t_{K^*(892)^+}(M_{12}, M_{23}) + (1 \leftrightarrow 2), \quad (25)$$

where the amplitude $t(M_{12})|_{K_S^0 K_S^0 \pi^+}$ is given by Eq. (14), the one $t_{K^*(892)^+}(M_{12}, M_{23})$ by Eq. (22), and $(1 \leftrightarrow 2)$ resembles the symmetry between the two identical K_S^0 in the final states. With Eq. (24), one can easily obtain the invariant mass spectra $d\Gamma/dM_{12}$, $d\Gamma/dM_{13}$ and $d\Gamma/dM_{23}$ by integrating over each of the invariant mass variables with the limits of the Dalitz plot, more details can be found in the PDG [61].

III. RESULTS

For the regularization scale μ in the loop functions, see Eq. (15), it is normal to set its value as $\mu = 0.6$ GeV for the pseudoscalar-pseudoscalar interaction [14,81,88,93,98] and $\mu = 1.0$ GeV for the vector-vector meson interaction [44], respectively. One should keep in mind that a_μ and μ are not independent; see more discussions in Ref. [99]. Thus, in our formalism, due to including the interactions between the pseudoscalar and vector mesons, we take μ as a free parameter. Thus, in our theoretical formalism, there are eleven parameters: μ is the regularization scale in the

loop functions, C_i ($i = 1, 2, \dots, 8$) are the free parameters in S -wave interaction amplitude, D and $\alpha_{K^*(892)^+}$ are the production factor and phase appearing in the P -wave amplitude. We can obtain these parameters by doing a combined fit to the invariant mass distributions of the $D_s^+ \rightarrow K_S^0 K_S^0 \pi^+$ decay reported by the BESIII collaboration [57]. The values of these parameters are given in Table I, where the fitted $\chi^2/\text{d.o.f.} = 175.97/(80 - 11) = 2.55$. With these fitted parameters, the obtained results of the $K_S^0 K_S^0$ and $K_S^0 \pi^+$ invariant mass distributions are shown in Fig. 6, where the error bands are not so visible. In fact, even though the parameters are correlated with each other much due to the interference effect, see Eq. (25), as one can see from Table I the error of μ is less than 2%, which is dominant and leads to such small error band. Indeed, in the two-body interaction amplitude, the theoretical uncertainties mainly come from the value of μ in the loop, which affects the peak position. Besides, the errors of the data are small, which give strong constraint on the fit, and thus, there is not much freedom to the fit results. For the regularization scale, a value $\mu = 0.648$ GeV is gotten from the fit, see Table I, and then, the subtraction constants a_μ for the corresponding coupled channels can be calculated by Eq. (16), obtained as

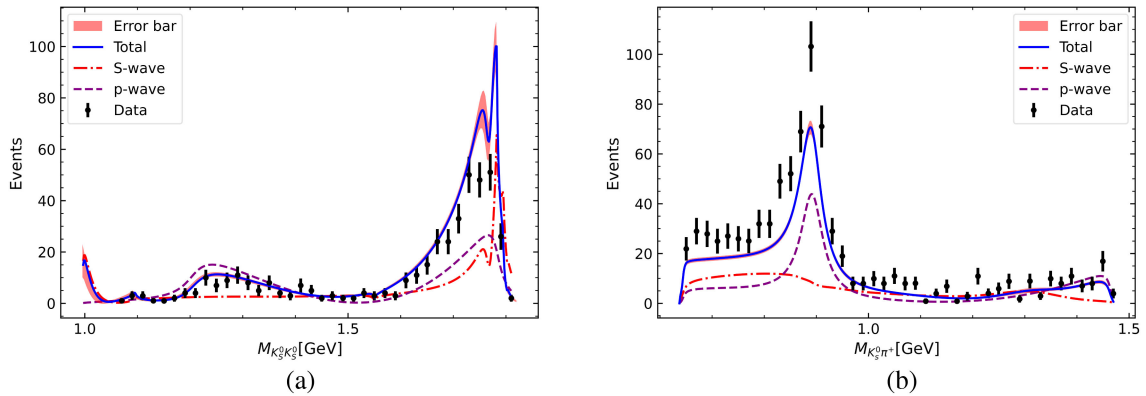


FIG. 6. Combined fit for the invariant mass distributions of the decay $D_s^+ \rightarrow K_S^0 K_S^0 \pi^+$. (a) Invariant mass distribution of $K_S^0 K_S^0$. (b) Invariant mass distribution of $K_S^0 \pi^+$. The solid (blue) lines are the total contributions of the S and P waves, the dashed (purple) lines represent the contribution of the $K^*(892)^+$, the dashed-dotted (red) lines are the contributions from the S -wave interactions with the resonances $S(980)$ and $S(1710)$. The dotted (black) points are the experimental data measured by the BESIII collaboration [57].

$$\begin{aligned}
 a_{K^+K^+} &= -1.99, & a_{K^*0\bar{K}^*0} &= -1.99, & a_{\rho^0\omega} &= -1.89, & a_{\rho^0\phi} &= -2.10, & a_{K^+K^-} &= -1.63, \\
 a_{K^0\bar{K}^0} &= -1.63, & a_{\pi^0\eta} &= -1.67, & a_{\rho^+\rho^-} &= -1.88, & a_{\rho^0\rho^0} &= -1.88, & a_{\omega\omega} &= -1.89, \\
 a_{\omega\phi} &= -2.10, & a_{\phi\phi} &= -2.10, & a_{\pi^+\pi^-} &= -1.41, & a_{\pi^0\pi^0} &= -1.41, & a_{\eta\eta} &= -1.67.
 \end{aligned} \tag{26}$$

For the $K_S^0 K_S^0$ invariant mass distributions as shown in Fig. 6(a), the bumps around 1.3 GeV benefit from the contribution of the $K^*(892)^+$ resonance, see the results of the dashed (purple) line, which also contributes to the region of 1.6–1.8 GeV. In Fig. 6(a), our fitting for the obvious resonance structure around 1.7 GeV is a bit higher than the data, see the results of the solid (blue) line, which also splits into two overlapped peaks due to the mixing effect of the $a_0(1710)$ and $f_0(1710)$ generated from the S -wave amplitude, and where it is difficult to fit well from our different tests, even though there are eight parameters in the S -wave amplitude; also see the discussions later. Furthermore, an obvious enhancement around the $K_S^0 K_S^0$ threshold is caused by the resonances $S(980)$, which are also dynamically generated in the S -wave final state interactions. Then, using the obtained results of the a_μ for each couple channel, see Eq. (26), we calculate the corresponding poles for the $a_0(980)$, $f_0(980)$, $a_0(1710)$, and $f_0(1710)$ states in the complex Riemann sheets, which are listed in Table II. Since the pole is located at $(M + i\frac{\Gamma}{2})$, one can easily obtain the total width of the corresponding resonances. From Table II, the pole for the $a_0(980)$, $f_0(980)$, and $a_0(1710)$ states are not much different from our former results of Refs. [68,100]. However, the corresponding width of the $a_0(1710)$ is several times smaller than those obtained in Refs. [44,45,66]. Note that there is a difference of about 30 MeV between the poles of $a_0(1710)$ and $f_0(1710)$, which with the small widths causes the split structure at the high energy region around 1.7 GeV in the $K_S^0 K_S^0$ mass distributions as discussed above. Similarly, for the $K_S^0 \pi^+$ mass distribution as shown in Fig. 6(b), the contribution from the state $K^*(892)^+$ enhances in the energy region around 0.8 and 1.0 GeV, while the S -wave amplitude mainly contributes to the low-energy region. In Fig. 6(b), one can see that there are obvious discrepancies between our fit and experimental data. After checking carefully, we find that the data of the bumps around

1.3 GeV in Fig. 6(a), which suppress the P -wave amplitude of the $K^*(892)^+$ with the destroyed interference effect from the S -wave amplitude, also prevent the fitting results of Fig. 6(b). To reveal this suppression effect, we fit only the data of the invariant mass distribution of $K_S^0 K_S^0$, as shown the results in Fig. 7. As seen from Fig. 7, there are two obvious peaks in the energy region of 1.7 GeV in Fig. 7(a), which come from the contribution of the S -wave amplitude and show more clear mixing effect, and the data of the $K_S^0 \pi^+$ spectrum in Fig. 7(b) is also described not bad with the fitted parameters and similar to what we get in Fig. 6(b). Note that using the fitting results of Fig. 7, the extracted poles and branching ratios are not much different from the results of Table II and Eq. (30) later.

As one can see from Figs. 6 and 7, the mixing signals of the $a_0(980)$ - $f_0(980)$ and $a_0(1710)$ - $f_0(1710)$ states are clearly shown, especially for the one of the $a_0(1710)$ - $f_0(1710)$ states, where two overlap peaks are found due to the 30 MeV mass differences between their poles. As shown in Eq. (14), the final state interaction amplitude has the contributions of the two-body interaction amplitudes $T_{K^+K^- \rightarrow K^0\bar{K}^0}$, $T_{K^0\bar{K}^0 \rightarrow K^0\bar{K}^0}$ and $T_{K^+K^+ \rightarrow K^0\bar{K}^0}$, $T_{K^*0\bar{K}^*0 \rightarrow K^0\bar{K}^0}$ with the coefficients C_1, C_2 and C_4, C_5 , respectively. In fact, these amplitudes contain the components of both isospin $I = 0$ and $I = 1$, decomposed as

$$T_{K^+K^- \rightarrow K^0\bar{K}^0} = \frac{1}{2}(T_{K\bar{K} \rightarrow K\bar{K}}^{I=0} - T_{K\bar{K} \rightarrow K\bar{K}}^{I=1}), \tag{27}$$

$$T_{K^0\bar{K}^0 \rightarrow K^0\bar{K}^0} = \frac{1}{2}(T_{K\bar{K} \rightarrow K\bar{K}}^{I=0} + T_{K\bar{K} \rightarrow K\bar{K}}^{I=1}), \tag{28}$$

which are similar for the channels $K^{*+}K^{*-}$ and $K^{*0}\bar{K}^{*0}$. From the fit results of Table I, one can find that the parameters $C_1 \neq C_2$ and $C_4 \neq C_5$, and thus, the final results will have the contributions of the amplitudes of both $T^{I=0}$ and $T^{I=1}$, where the f_0 and a_0 states are generated, respectively. Thus, this leads to the consequence of the

TABLE II. Poles compared with the other works (unit: GeV).

Parameters	This work	Ref. [68]	Ref. [100]	Ref. [44]	Ref. [66]	Ref. [45]
	$\mu = 0.648$	$\mu = 0.716$	$q_{\max} = 0.931$	$\mu = 1.0$	$q_{\max} = 1.0$	$q_{\max} = 1.0$
$a_0(980)$	$1.0598 + 0.024i$	$1.0419 + 0.0345i$	$1.0029 + 0.0567i$
$f_0(980)$	$0.9912 + 0.003i$...	$0.9912 + 0.0135i$
$a_0(1710)$	$1.7981 + 0.0018i$	$1.7936 + 0.0094i$...	$1.780 - 0.066i$	$1.72 - 0.010i$	$1.76 \pm 0.03i$
$f_0(1710)$	$1.7676 + 0.0093i$	$1.726 - 0.014i$

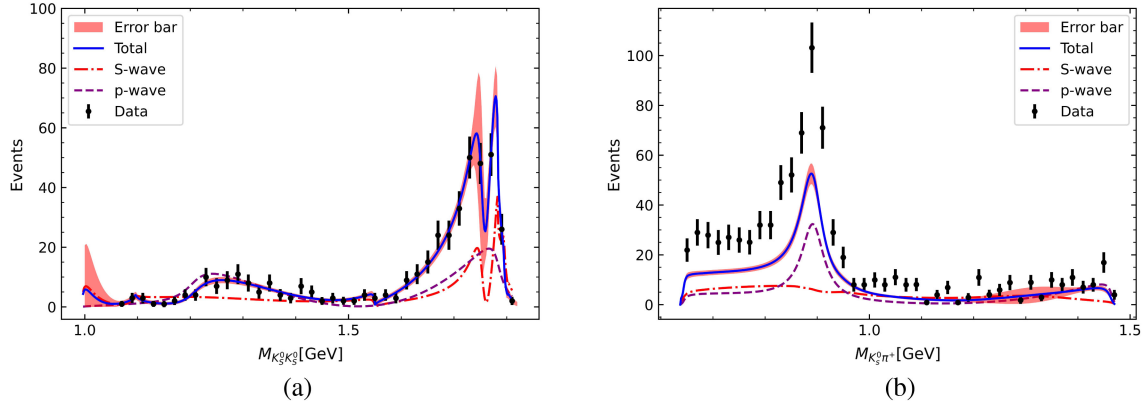


FIG. 7. Fit only for the data of the $K_S^0 K_S^0$ spectrum. (a) Invariant mass distribution of $K_S^0 K_S^0$. (b) Invariant mass distribution of $K_S^0 \pi^+$. Others are the same as Fig. 6.

mixing effect of the a_0 - f_0 states. More discussions on the a_0 - f_0 mixing under the dynamic of the amplitudes with the physical basis can be found in our former work [101].

Besides, we also calculate the ratios of branching fractions for the corresponding decay channels based on our fitting results. By integrating the $K_S^0 K_S^0$ and $K_S^0 \pi^+$ invariant mass distributions, we can get the ratios as below:

$$\frac{\mathcal{B}(D_s^+ \rightarrow S(980)\pi^+, S(980) \rightarrow K_S^0 K_S^0)}{\mathcal{B}(D_s^+ \rightarrow K_S^0 K^*(892)^+, K^*(892)^+ \rightarrow K_S^0 \pi^+)} = 0.122^{+0.032}_{-0.023},$$

$$\frac{\mathcal{B}(D_s^+ \rightarrow S(1710)\pi^+, S(1710) \rightarrow K_S^0 K_S^0)}{\mathcal{B}(D_s^+ \rightarrow K_S^0 K^*(892)^+, K^*(892)^+ \rightarrow K_S^0 \pi^+)} = 0.552^{+0.460}_{-0.297},$$
(29)

$$\mathcal{B}(D_s^+ \rightarrow S(980)\pi^+, \quad S(980) \rightarrow K_S^0 K_S^0) = (0.36 \pm 0.04^{+0.10}_{-0.06}) \times 10^{-3},$$

$$\mathcal{B}(D_s^+ \rightarrow S(1710)\pi^+, \quad S(1710) \rightarrow K_S^0 K_S^0) = (1.66 \pm 0.17^{+1.38}_{-0.89}) \times 10^{-3},$$
(30)

where the first uncertainties are estimated from the errors of experimental results, and the second ones are from Eq. (29). Compared with the experimental results, our results of the branching fraction for the decay ($D_s^+ \rightarrow S(1710)\pi^+, S(1710) \rightarrow K_S^0 K_S^0$) is about 1/2 of the measurements [57], $(3.1 \pm 0.3 \pm 0.1) \times 10^{-3}$. Meanwhile, we also evaluate the branching fraction of the resonance $S(980)$, of which the value is $(0.36 \pm 0.04^{+0.10}_{-0.06}) \times 10^{-3}$. Note that, in principle, using Eqs. (27) and (28), one can separate the contributions from the isospin $I=0$ and $I=1$, where the states f_0 and a_0 are dynamically generated. Because of the a_0 - f_0 mixing effect with the strong interference between the two-body amplitudes, see

where we make a cut at 1.5 GeV for the lower contributions of the $S(1710)$. Therefore, for the $D_s^+ \rightarrow S(1710)\pi^+$ decay channel, the integration limits are chosen from 1.5 to 1.77 GeV, and the uncertainties are due to the limits 1.5 ± 0.05 and 1.77 ± 0.05 GeV. Then the integration limits for the $D_s^+ \rightarrow S(980)\pi^+$ processes are chosen from the corresponding threshold to 1.1 GeV, and for the $D_s^+ \rightarrow K^*(892)^+ K_S^0$ processes the limits are taken from 0.8 to 1.1 GeV. The uncertainties come from the changes of upper limits, which for both processes are around 1.1 ± 0.05 GeV. Thus, taking the branching fraction $\mathcal{B}(D_s^+ \rightarrow K^*(892)^+ K_S^0 \rightarrow K_S^0 K_S^0 \pi^+) = (3.0 \pm 0.3 \pm 0.1) \times 10^{-3}$ measured by the BESIII collaboration [57] as the input, we evaluate the branching fractions for other processes,

Eq. (25), we cannot extract the branching ratios of $f_0(980)/f_0(1710) \rightarrow K_S^0 K_S^0$ and $a_0(980)/a_0(1710) \rightarrow K_S^0 K_S^0$ alone. Furthermore, for the lack of the experimental measurements, no more available information from the PDG [61] can be compared with our results.

IV. SUMMARY

Inspired by an enhancement near 1.7 GeV observed in the $K_S^0 K_S^0$ mass spectrum of the decay $D_s^+ \rightarrow K_S^0 K_S^0 \pi^+$, which was reported by the BESIII collaboration, we study this decay process exploiting the final state interaction approach based on the coupled channel interaction. The

resonances $S(980)$ and $S(1710)$ are dynamically generated from the S -wave coupled channel interactions. Moreover, we consider the contribution of the intermediate resonance $K^*(892)^+$ in P wave, which plays a key role in shaping $K_S^0\pi^+$ mass distribution. With the contributions from both the S -wave and P -wave amplitudes, we make a combined fit of two invariant mass spectra of $K_S^0K_S^0$ and $K_S^0\pi^+$, where one can determine the free parameters of our formalism and get a good description of the experimental data. With the obtained parameters, we calculated the pole of the states $a_0(980)$, $f_0(980)$, $a_0(1710)$, and $f_0(1710)$ in the complex Riemann sheets, which are consistent with our former results. Note that the poles for the $a_0(1710)$ and $f_0(1710)$ have a difference of about 30 MeV, which shows a mixing effect to the enhancement around 1.7 GeV of the $K_S^0K_S^0$ invariant mass distribution, but with some uncertainties due to the small widths of the poles. Furthermore, we calculate the branching fractions of related decay channels, where the one for the decay $D_s^+ \rightarrow S(1710)\pi^+ \rightarrow K_S^0K_S^0\pi^+$ is smaller than the measurement, and a prediction of the

process $D_s^+ \rightarrow S(980)\pi^+ \rightarrow K_S^0K_S^0\pi^+$ is made, which can be measured in future experiments.

ACKNOWLEDGMENTS

We acknowledge Professor Eulogio Oset for careful reading of the manuscript and useful comments, and Professor En Wang for helpful comments. This work is supported by the Fundamental Research Funds for the Central Universities of Central South University under Grants No. 1053320214315 and No. 2022ZZTS0169, and the Postgraduate Scientific Research Innovation Project of Hunan Province under No. CX20220255, and partly by the Natural Science Foundation of Changsha under Grant No. kq2208257, the Natural Science Foundation of Hunan Province under Grant No. 2023JJ30647, the Natural Science Foundation of Guangxi Province under Grant No. 2023JJA110076, and the National Natural Science Foundation of China under Grants No. 12365019 and No. 12275364.

-
- [1] A. Astier, L. Montanet, M. Baubillier, and J. Duboc, *Phys. Lett.* **25B**, 294 (1967).
 - [2] R. Ammar R. Davis, W. Kropac, J. Mott, D. Slate, B. Werner, M. Derrick, T. Fields, and F. Schweingruber, *Phys. Rev. Lett.* **21**, 1832 (1968).
 - [3] C. Defoix, P. Rivet, J. Sjaud, B. Conforto, M. Widgoff, and F. Shively, *Phys. Lett.* **28B**, 353 (1968).
 - [4] S. Godfrey and N. Isgur, *Phys. Rev. D* **32**, 189 (1985).
 - [5] D. Morgan and M. R. Pennington, *Z. Phys. C* **48**, 623 (1990).
 - [6] R. L. Jaffe, *Phys. Rev. D* **15**, 267 (1977).
 - [7] N. N. Achasov, S. A. Devyanin, and G. N. Shestakov, *Phys. Lett.* **96B**, 168 (1980).
 - [8] K. L. Au, M. R. Pennington, and D. Morgan, *Phys. Lett.* **167B**, 229 (1986).
 - [9] S. M. Flatté, *Phys. Lett.* **63B**, 224 (1976).
 - [10] J. D. Weinstein and N. Isgur, *Phys. Rev. Lett.* **48**, 659 (1982).
 - [11] B. S. Zou and D. V. Bugg, *Phys. Rev. D* **50**, 591 (1994).
 - [12] G. Janssen, B. C. Pearce, K. Holinde, and J. Speth, *Phys. Rev. D* **52**, 2690 (1995).
 - [13] N. A. Tornqvist and M. Roos, *Phys. Rev. Lett.* **76**, 1575 (1996).
 - [14] J. A. Oller and E. Oset, *Nucl. Phys.* **A620**, 438 (1997); **652**, 407(E) (1999).
 - [15] M. P. Locher, V. E. Markushin, and H. Q. Zheng, *Eur. Phys. J. C* **4**, 317 (1998).
 - [16] J. A. Oller, E. Oset, and J. R. Pelaez, *Phys. Rev. D* **59**, 074001 (1999); **60**, 099906(E) (1999); **75**, 099903(E) (2007).
 - [17] J. A. Oller, E. Oset, and J. R. Pelaez, *Phys. Rev. Lett.* **80**, 3452 (1998).
 - [18] N. N. Achasov, S. A. Devyanin, and G. N. Shestakov, *Phys. Lett.* **88B**, 367 (1979).
 - [19] B. Kerbikov and F. Tabakin, *Phys. Rev. C* **62**, 064601 (2000).
 - [20] F. E. Close and A. Kirk, *Phys. Lett. B* **489**, 24 (2000).
 - [21] V. Y. Grishina, L. A. Kondratyuk, M. Buescher, W. Cassing, and H. Stroher, *Phys. Lett. B* **521**, 217 (2001).
 - [22] N. N. Achasov and A. V. Kiselev, *Phys. Lett. B* **534**, 83 (2002).
 - [23] A. E. Kudryavtsev, V. E. Tarasov, J. Haidenbauer, C. Hanhart, and J. Speth, *Phys. Rev. C* **66**, 015207 (2002).
 - [24] N. N. Achasov and G. N. Shestakov, *Phys. Rev. Lett.* **92**, 182001 (2004).
 - [25] J. J. Wu, Q. Zhao, and B. S. Zou, *Phys. Rev. D* **75**, 114012 (2007).
 - [26] C. Hanhart, B. Kubis, and J. R. Peláez, *Phys. Rev. D* **76**, 074028 (2007).
 - [27] J. J. Wu and B. S. Zou, *Phys. Rev. D* **78**, 074017 (2008).
 - [28] M. Ablikim *et al.* (BESIII Collaboration), *Phys. Rev. D* **83**, 032003 (2011).
 - [29] M. Ablikim *et al.* (BESIII Collaboration), *Phys. Rev. Lett.* **121**, 022001 (2018).
 - [30] A. Etkin, K. J. Foley, R. S. Longacre, W. A. Love, T. W. Morris, S. Ozaki, E. D. Platner, V. A. Polychronakos, A. C. Saulys, Y. Teramoto *et al.*, *Phys. Rev. D* **25**, 1786 (1982).
 - [31] C. Edwards, R. Partridge, C. Peck, F. Porter, D. Antreasyan, Y. F. Gu, W. S. Kollmann, M. Richardson,

- K. Strauch, K. Wacker *et al.*, *Phys. Rev. Lett.* **48**, 458 (1982).
- [32] J. Segovia, D. R. Entem, and F. Fernandez, *Phys. Lett. B* **662**, 33 (2008).
- [33] F. E. Close and Q. Zhao, *Phys. Rev. D* **71**, 094022 (2005).
- [34] F. Giacosa, T. Gutsche, V. E. Lyubovitskij, and A. Faessler, *Phys. Rev. D* **72**, 094006 (2005).
- [35] H. Y. Cheng, C. K. Chua, and K. F. Liu, *Phys. Rev. D* **74**, 094005 (2006).
- [36] M. Albaladejo and J. A. Oller, *Phys. Rev. Lett.* **101**, 252002 (2008).
- [37] L. C. Gui Y. Chen, G. Li, C. Liu, Y.-B. Liu, J.-P. Ma, Y.-B. Yang, and J.-B. Zhang (CLQCD Collaboration), *Phys. Rev. Lett.* **110**, 021601 (2013).
- [38] A. H. Fariborz, A. Azizi, and A. Asrar, *Phys. Rev. D* **92**, 113003 (2015).
- [39] S. Janowski, F. Giacosa, and D. H. Rischke, *Phys. Rev. D* **90**, 114005 (2014).
- [40] J. M. Frère and J. Heeck, *Phys. Rev. D* **92**, 114035 (2015).
- [41] M. Ablikim *et al.* (BESIII Collaboration), *Phys. Rev. Lett.* **129**, 192002 (2022).
- [42] M. Chanowitz, *Phys. Rev. Lett.* **95**, 172001 (2005).
- [43] K. T. Chao, X. G. He, and J. P. Ma, *Phys. Rev. Lett.* **98**, 149103 (2007).
- [44] L. S. Geng and E. Oset, *Phys. Rev. D* **79**, 074009 (2009).
- [45] M. L. Du, D. Gülmez, F. K. Guo, U.-G. Meißner, and Q. Wang, *Eur. Phys. J. C* **78**, 988 (2018).
- [46] Z. L. Wang and B. S. Zou, *Phys. Rev. D* **104**, 114001 (2021).
- [47] H. Nagahiro, L. Roca, E. Oset, and B. S. Zou, *Phys. Rev. D* **78**, 014012 (2008).
- [48] T. Branz, L. S. Geng, and E. Oset, *Phys. Rev. D* **81**, 054037 (2010).
- [49] L. S. Geng, F. K. Guo, C. Hanhart, R. Molina, E. Oset, and B. S. Zou, *Eur. Phys. J. A* **44**, 305 (2010).
- [50] W. L. Wang and Z. Y. Zhang, *Phys. Rev. C* **84**, 054006 (2011).
- [51] A. Martinez Torres, K. P. Khemchandani, F. S. Navarra, M. Nielsen, and E. Oset, *Phys. Lett. B* **719**, 388 (2013).
- [52] J. J. Xie and E. Oset, *Phys. Rev. D* **90**, 094006 (2014).
- [53] L. R. Dai, J. J. Xie, and E. Oset, *Phys. Rev. D* **91**, 094013 (2015).
- [54] R. Molina, L. R. Dai, L. S. Geng, and E. Oset, *Eur. Phys. J. A* **56**, 173 (2020).
- [55] J. P. Lees *et al.* (BABAR Collaboration), *Phys. Rev. D* **104**, 072002 (2021).
- [56] J. P. Lees *et al.* (BABAR Collaboration), *Phys. Rev. D* **97**, 112006 (2018).
- [57] M. Ablikim *et al.* (BESIII Collaboration), *Phys. Rev. D* **105**, L051103 (2022).
- [58] P. del Amo Sanchez *et al.* (BABAR Collaboration), *Phys. Rev. D* **83**, 052001 (2011).
- [59] M. Ablikim *et al.* (BESIII Collaboration), *Phys. Rev. D* **104**, 012016 (2021).
- [60] M. Ablikim *et al.* (BESIII Collaboration), *Phys. Rev. Lett.* **129**, 182001 (2022).
- [61] R. L. Workman *et al.* (Particle Data Group), *Prog. Theor. Exp. Phys.* **2022**, 083C01 (2022).
- [62] M. Ablikim *et al.* (BES Collaboration), *Phys. Lett. B* **607**, 243 (2005).
- [63] A. Martinez Torres, K. P. Khemchandani, D. Jido, and A. Hosaka, *Phys. Rev. D* **84**, 074027 (2011).
- [64] A. V. Anisovich, D. V. Bugg, V. A. Nikonov, A. V. Sarantsev, and V. V. Sarantsev, *Phys. Rev. D* **85**, 014001 (2012).
- [65] D. Guo, W. Chen, H. X. Chen, X. Liu, and S. L. Zhu, *Phys. Rev. D* **105**, 114014 (2022).
- [66] Z. L. Wang and B. S. Zou, *Eur. Phys. J. C* **82**, 509 (2022).
- [67] X. Zhu, H. N. Wang, D. M. Li, E. Wang, L. S. Geng, and J. J. Xie, *Phys. Rev. D* **107**, 034001 (2023).
- [68] Z. Y. Wang, Y. W. Peng, J. Y. Yi, W. C. Luo, and C. W. Xiao, *Phys. Rev. D* **107**, 116018 (2023).
- [69] L. R. Dai, E. Oset, and L. S. Geng, *Eur. Phys. J. C* **82**, 225 (2022).
- [70] X. Zhu, D. M. Li, E. Wang, L. S. Geng, and J. J. Xie, *Phys. Rev. D* **105**, 116010 (2022).
- [71] Y. Ding, X. H. Zhang, M. Y. Dai, E. Wang, D. M. Li, L. S. Geng, and J. J. Xie, *Phys. Rev. D* **108**, 114004 (2023).
- [72] Y. Ding, E. Wang, D. M. Li, L. S. Geng, and J. J. Xie, *arXiv:2401.17322*.
- [73] N. N. Achasov and G. N. Shestakov, *Phys. Rev. D* **108**, 036018 (2023).
- [74] E. Oset, L. R. Dai, and L. S. Geng, *Sci. Bull.* **68**, 243 (2023).
- [75] L. L. Chau and H. Y. Cheng, *Phys. Rev. D* **36**, 137 (1987).
- [76] L. L. Chau, *Phys. Rep.* **95**, 1 (1983).
- [77] R. J. Morrison and M. S. Witherell, *Annu. Rev. Nucl. Part. Sci.* **39**, 183 (1989).
- [78] H. A. Ahmed, Z. Y. Wang, Z. F. Sun, and C. W. Xiao, *Eur. Phys. J. C* **81**, 695 (2021).
- [79] W. H. Liang, J. J. Xie, and E. Oset, *Eur. Phys. J. C* **75**, 609 (2015).
- [80] W. F. Wang, A. Feijoo, J. Song, and E. Oset, *Phys. Rev. D* **106**, 116004 (2022).
- [81] W. H. Liang and E. Oset, *Phys. Lett. B* **737**, 70 (2014).
- [82] G. Toledo, N. Ikeno, and E. Oset, *Eur. Phys. J. C* **81**, 268 (2021).
- [83] J. A. Oller and U.-G. Meißner, *Phys. Lett. B* **500**, 263 (2001).
- [84] J. A. Oller and E. Oset, *Phys. Rev. D* **60**, 074023 (1999).
- [85] D. Gamermann, E. Oset, D. Strottman, and M. J. Vicente Vacas, *Phys. Rev. D* **76**, 074016 (2007).
- [86] L. Alvarez-Ruso, J. A. Oller, and J. M. Alarcon, *Phys. Rev. D* **82**, 094028 (2010).
- [87] Z. H. Guo, L. Liu, U.-G. Meißner, J. A. Oller, and A. Rusetsky, *Phys. Rev. D* **95**, 054004 (2017).
- [88] M. Y. Duan, J. Y. Wang, G. Y. Wang, E. Wang, and D. M. Li, *Eur. Phys. J. C* **80**, 1041 (2020).
- [89] Z. Y. Wang, H. A. Ahmed, and C. W. Xiao, *Phys. Rev. D* **105**, 016030 (2022).
- [90] Z. H. Guo, L. Liu, U.-G. Meißner, J. A. Oller, and A. Rusetsky, *Eur. Phys. J. C* **79**, 13 (2019).
- [91] E. Oset and A. Ramos, *Nucl. Phys. A* **635**, 99 (1998).
- [92] X. Z. Ling, M. Z. Liu, J. X. Lu, L. S. Geng, and J. J. Xie, *Phys. Rev. D* **103**, 116016 (2021).
- [93] Z. Y. Wang, J. Y. Yi, Z. F. Sun, and C. W. Xiao, *Phys. Rev. D* **105**, 016025 (2022).
- [94] M. Bando, T. Kugo, S. Uehara, K. Yamawaki, and T. Yanagida, *Phys. Rev. Lett.* **54**, 1215 (1985).

- [95] M. Bando, T. Kugo, and K. Yamawaki, *Phys. Rep.* **164**, 217 (1988).
- [96] R. Molina, D. Nicmorus, and E. Oset, *Phys. Rev. D* **78**, 114018 (2008).
- [97] L. Roca and E. Oset, *Phys. Rev. D* **103**, 034020 (2021).
- [98] J. M. Dias, F. S. Navarra, M. Nielsen, and E. Oset, *Phys. Rev. D* **94**, 096002 (2016).
- [99] A. Ozpineci, C. W. Xiao, and E. Oset, *Phys. Rev. D* **88**, 034018 (2013).
- [100] H. A. Ahmed and C. W. Xiao, *Phys. Rev. D* **101**, 094034 (2020).
- [101] C. W. Xiao, U.-G. Meißner, and J. A. Oller, *Eur. Phys. J. A* **56**, 23 (2020).